Journal homepage https://sjpas.univsul.edu.iq
Sulaimani Journal for Pure and Applied Sciences
ISSN:1812-4100

Original Article

Petrogenetic Processes in Andesite Generation: Insights from Walash Volcanic Arc

Jabbar M. A. Qaradaghi [a, *]

[a] *Department of Earth Sciences and Petroleum, College of Science, University of Sulaimani, Sulaimani city, Kurdistan Region of Iraq.*

ARTICLE INFO

Article History:
Received: 1/10/2025
Revised: 20/11/2025
Accepted: 15/12/2025
Published online: 25/12/2025

Key Words:
Andesites
Adakite
ICP-MS
Petrogenesis
Subduction zone
Walash Volcanics

ABSTRACT

Andesites are characteristic rocks of subduction zone magmatism. Andesitic rocks investigated from Walash Volcanics (WV) throughout field, petrological, mineralogical, and geochemical aspects, classifying into two types pyroxene-rich (px-andesite) and hornblende-rich (hbl-andesite). This study is the first to report well-formed magmatic hornblende crystals in andesitic rocks from the Mawat area in Iraqi Kurdistan. Andesites, in WV, are comprised of plagioclase, pyroxene, and hornblende phenocrysts along with a groundmass of plagioclase, hematite, and sanidine. XRD examination indicates that the plagioclase grains are predominantly composed of albite. Andesitic rock samples (px-andesite and hbl-andesite) show typical porphyritic and magmatic flow textures. The primary alteration product includes sericite after plagioclase. ICP-MS analysis shows that andesitic rock samples tend to be high-Mg andesites, and their magma formed out of the field of mantle-derived melts. Furthermore, hbl-andesite rock samples represent normal calc-alkaline andesites, while the px-andesites represent the andesites from more mature arcs. Geochemical discriminations based on diagnostic trace elemental ratios indicate that the pyroxene and hornblende andesites both formed within a volcanic arc tectonic setting. The px-andesite exhibit compositions proximal to the average continental crust and align with magmas from a normal island arc with fractionation trends dominated by plagioclase. In contrast, the hbl-andesite reveals a distinct adakitic signature, characterized by elevated Sr/Y and La/Yb ratios, and their compositional trends are consistent with a fractionation process controlled by hornblende and pyroxene. This geochemical contradiction suggests two different petrogenetic pathways: firstly, the px-andesites likely originated from typical mantle wedge melting, secondly the adakitic nature of the hbl-andesites may be derived from partial melting of a subducted slab or assimilation of lower crustal material.

OPEN ACCESS

1. Introduction

Subduction zone magmas are the primary ingredient for growth of the continental crust, making andesites a characteristic of magmatism in subduction zone (Davidson et al., 2007; Reubi & Müntener, 2022). To understand the origins of continental crust and subduction zone magmatism, one must have a solid understanding of andesite. Andesite, with intermediate volcanic rock of SiO_2 content (54–63 %), is the dominant rock in many contemporary volcanic arcs. Andesite offers important information about the processes that generate magma close to convergent margins (Kelemen, 1995; Kelemen et al., 2003; Gill, 2012; Gill & Fitton, 2022). Current models have suggested

* Corresponding author.
E-mail address: jabbar.faraj@univsul.edu.iq (J. Qaradaghi)

several possible formations, such as: (1) partial melting of metabasaltic crust; (2) mixing between felsic and mafic end-member magmas; (3) hybridization of mantle peridotite with melts derived from slabs; and (4) fractional crystallization of basaltic parent magmas (Tatsumi & Eggins, 1995; Mibe et al., 2011; Cassidy et al., 2015; Qaradaghi et al., 2019; Straub et al., 2020; Chen et al., 2021).

Generally, andesite petrogenesis involves complex interaction between subducted oceanic plates, overlaying mantle materials, and the geochemical development of magmas produced by these processes. Recent studies emphasized that andesites are primarily the result of partial melting of subducting slabs, combined with assimilating components from both the mantle wedge and the continental crust. For example, Zhang et al. (2022) suggested a two-stage melting model in which subducted sediments first produce silicate-rich melts that then interact with the mantle wedge, supporting the idea that subducted components have a considerable influence on andesite composition. likewise, Ruiz-Mendoza et al. (2021) demonstrated that down going slabs associated with subduction-related magmatism contributed to the genesis of basaltic andesites in their study, highlighting the crucial role that slab-derived fluids and melts play in enriching the mantle source (Ruiz-Mendoza et al., 2021).

Furthermore, the fluid-induced melting and the incorporation of crustal materials into the melting regime both contribute to the formation of high-magnesium andesites that are typical of subduction zones, highlighting the significance of sediment recycling in these environments (Gao et al., 2022). Furthermore, andesitic magmas that erupt above subducted slabs show geochemical features consistent with formation from mantle peridotite under the influence of fluids released from the oceanic plates (Erdmann et al., 2019). Collectively, these results support the understanding that mantle interactions, slab-derived materials, and crustal assimilation all interact to form andesites in subduction zones, producing geochemically diverse andesitic magmas that reflect the complexity of subduction-related processes.

The Mawat area is a fascinating gallery for igneous rocks within a subduction zone setting. In addition, Walash volcano-sedimentary group (WVSg) is considered as a center of this gallery in adjacent to the Mawat Ophiolite complex (MOC). In general, a variety of igneous rocks within WVSg in the Kurdistan region have been investigated in terms of their field occurrences, geochemistry, and petrogenesis (Aziz, 1986; Koyi, 2009; Aswad et al., 2013; Qaradaghi & Mirza, 2023; Qaradaghi, 2024). While, in the Mawat area, andesites are the least studied rocks despite their importance in deciphering the geodynamic and geochemical evolution of the Walash volcanic arc. Thus, this work presents new insight through presenting a detailed geological, petrological, and geochemical data for the andesitic rocks of WV and integrating these data to constrain their petrogenesis as well as the tectonic setting of magmatism within this region. The main objectives of this paper are to introduce and classify in detail the andesitic rocks of WVSg in Mawat area. As well as, explain their petrogenesis by contradicting to the recent ideas and interpretation that refuse the magmatic rocks within Iraqi Zagros Thrust Zone (IZTZ).

2. Geology and Field Observations

The Walash volcanic group was referred to as the "Walash volcanic series" by Bolton, (1958). Walash hamlet in the northeastern Iraqi river valley of the Rowanduz is the type locality for this group. This group is composed primarily of volcanic rocks and is around 1000 meters thick in its type locality (Buday & Jassim, 1987; Jassim & Goff, 2006). While its thickness within the Mawat area is roughly around 4000 meters (Qaradaghi & Mirza, 2023; Qaradaghi, 2024). The volcanic cone that makes up the Walash volcanic group is encircled by sedimentary strata that may stretch up to 3500 meters beyond the type region (Bolton, 1958). Tectonically, the research area is situated inside the Cenozoic units of the Zagros Imbricate Zone (ZIZ) (Fig. 1a).

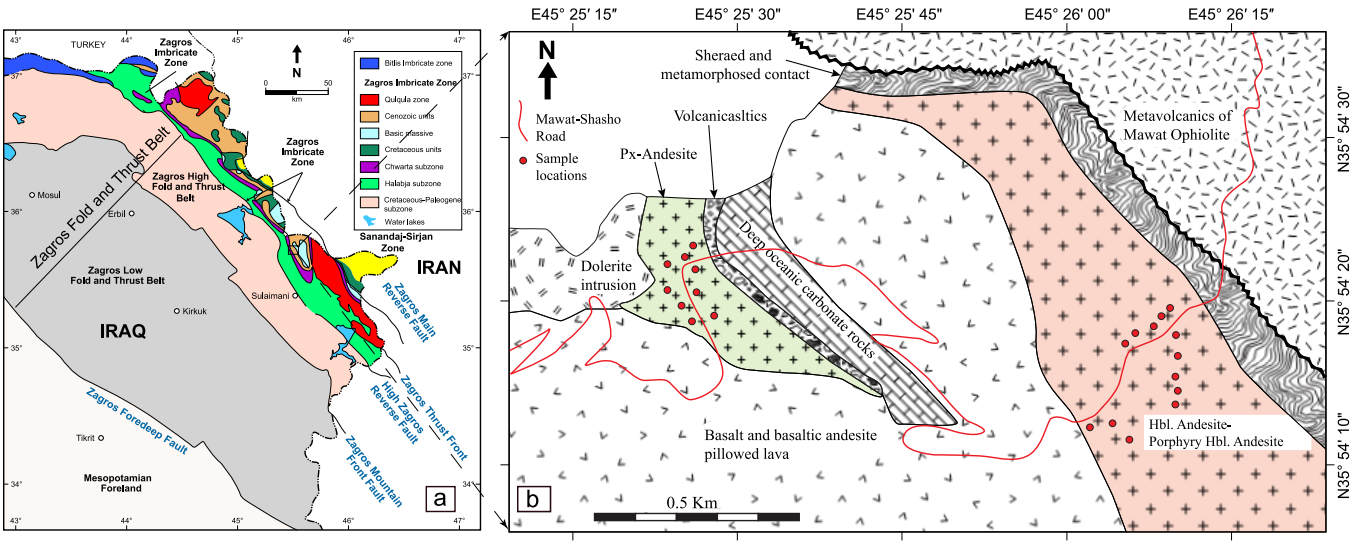

Figure 1. (a) Regional tectonic map of the Iraqi Kurdistan region, showing major tectonic subdivisions (Al-Kadhimi et al., 1996). Tectonic zones and boundaries are after (Al-Qayim et al., 2012; Mohammad et al., 2014). (b) Geological map of the studied Andesite and surrounding rocks within the Mawat area.

The studied area, lies within E45° 25' 15" – 45° 26' 15" and N35° 54' 00"- 35° 54' 30" (Fig. 1b), comprise various volcano-sedimentary rocks such as dolerite intrusions, basalt and basaltic andesite pillowed lava, 250 m deep-marine sedimentary strata, volcaniclastics, sheared and metamorphosed contact with Mawat Ophiolite Complex (MOC), and andesitic rocks (px-andesite and hbl-andesite). Andesitic rocks (selected rocks of this study) crop out in two different locations along Mawat Shasho road (Figs. 1b and 2). Px-andesite rock (around 75 m thick) samples are light grey in colour, exhibit volcanic texture with massive structure, and plagioclase phenocrysts couldn't see by naked eyes in the field (Fig. 2a). While hbl-andesite rock (around 100 m thick) samples are porphyry rocks with grey-black in colour, having porphyritic texture with massive structure, and plagioclase and hornblende phenocrysts seen by naked eyes and are about 3-5 mm in size (Fig. 2b and c). Stratigraphically, the andesitic rocks of the WVSg have a clear stratigraphic distribution in the Mawat area. As massive lava flows embedded in volcaniclastic rocks, the pyroxene andesites (px-andesites) comprise the middle volcanic series. These are covered by volcaniclastic rocks in the east, dolerite intrusions in the west, and basalts and basaltic pillowed lava in the south (Figs. 1b and 2a). In addition, hornblende andesites (hbl-andesites), which are usually found in the higher stratigraphic and geographical level with the massive flows that tend to make direct contact with the overlying metavolcanics of MOCs (Fig. 2c).

However, extreme caution must be emphasized for any future fieldwork in the study area. As the area remains heavily contaminated with unmarked landmines from the Iran-Iraq War, particularly around key outcrops and access routes. Thus, the authors advise that geological investigations should only be conducted in coordination with the villagers who are familiar with the area.

3. Sampling and Analytical Techniques

Ten fresh andesitic rock samples from two different outcrops in the study area for the whole rock geochemistry (major, trace and REE elements) at ALS Laboratories in Seville, Spain. Samples were slabbed and powdered at the University of Sulaimani. Sample locations are represented by Figure 1b, as red points which represent fresh sample locations from the two andesitic outcrops.

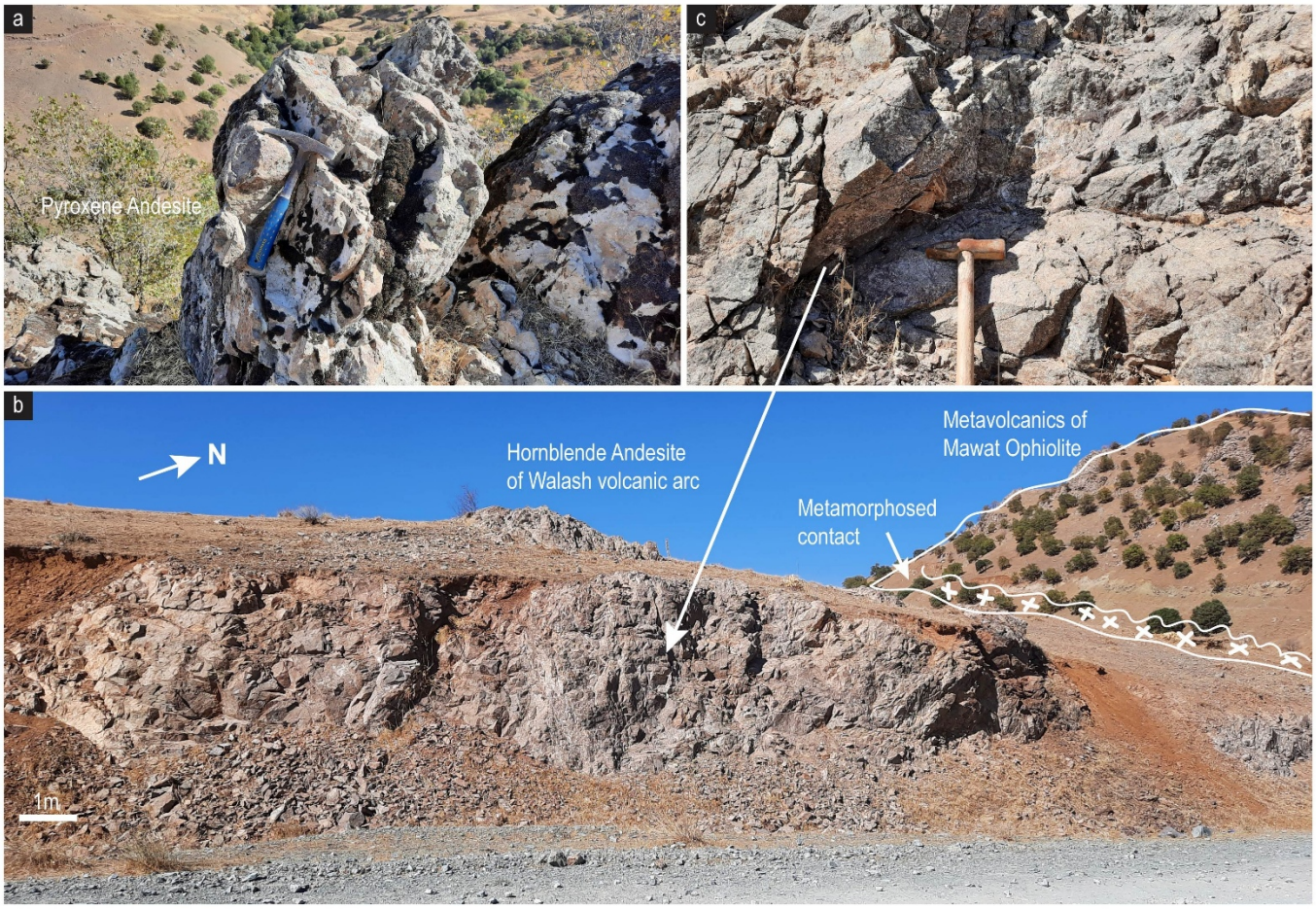

Figure 2. Field photo of the Andesite rocks and its contact with Mawat Ophiolite. (a) Pyroxene Andesite ridge, (b and c) Hornblende Andesite outcrop.

At the geology department Research Laboratories at the University of Sulaimani, the slabbed whole-rock samples were prepared with a water-cooled diamond-blade saw to remove (if) any weathered parts of the rock samples. All andesitic rock samples were powdered in hardened steel with a chromium-free tool steel vibrating cup mill by using a PULVERISETTE 9 machine at XRF research lab. Whole-rock powders were analysed by inductively coupled plasma-atomic emission spectroscopy (ICP-AES) and Mass spectrometer (ICP-MS) methods for major, trace, and rare earth element (REE) abundances in the ALS laboratories using geochemical procedures (ME-ICP06; ME-MS81; ME-4ACD81). For major and trace element analyses, structural water was removed from sample powders by heating in a furnace at 1000°C for 30 minutes. Loss on ignition (LOI) was determined from 1 gm of the powdered samples by heating in a furnace at 1000°C for 1 hour, and then the total weight change of the sample powder is calculated. Detection limits are <0.01% for major elements and 0.01-1 ppm for trace and REE elements, except for As and Cr, which have relative errors of 5 ppm. Mg numbers are calculated using the formula Mg# = [100 * MgO/ (MgO + Fe_2O_3) (molar)].

As well as two fresh samples have been selected for the mineralogical study. All rock samples were grounded into powders for X-ray diffraction analysis at the University of Sulaimani using a Panalytical X'Pert-Pro machine. The samples were scanned using a Cu (Anode Material) filter and K-Alpha1

radiation (1.541874 Å) at generator settings of 40 mA and 45 kV and recorded diffraction peaks are between 2Θ=5° and 2Θ=80°. Mineral patterns were identified using Match 3 software.

4. Results

4.1 Petrography

Phenocrysts in this study described for both px-andesite and hbl-andesite rock samples, have sizes > 300 µm (0.3 mm). While micro-phenocrysts are defined as crystal sizes between 300 and 100 µm (0.3-0.1 mm). The dominant phases for px-andesite rocks are plagioclase and pyroxene in order of their modal percentage (85% and 10%, respectively). Both plagioclase and pyroxene minerals appeared as either phenocrysts or micro-phenocrysts in the px-andesite rock samples. Generally, they are either subhedral laths or euhedral platy in habit. The px-andesite rock samples are characterized by pilotasitic texture, fine microlites of feldspar subparallel arranged in the groundmass, and trachytic texture (Fig. 3a and b). Hematite, which comprises 5% (modal), is regarded as a minor phase (Fig. 3a). Furthermore, in several rock samples of px-andesite, plagioclase exhibits a sieve or boxy cellular texture (Fig. 3c). The groundmass comprises micro-phenocrysts and microlites of plagioclase, pyroxene, and hematite minerals.

On the other hand, plagioclase and hornblende, with modal percentages of 60% and 30%, respectively, are the main phases in hbl-andesite rock samples (Fig. 3d-h). Other minor phases like hematite and sanidine comprise 10% of modal percentages (Fig. 3e and f). Phenocrysts, in hbl-andesite rock samples, are represented by plagioclase, hornblende, and sanidine minerals. Hornblende minerals are typical magmatic minerals that exhibit brown colour and euhedral form (six edges) (Fig. 3e and g). While plagioclase and sanidine are either euhedral lath or platy in habit (Fig. 3d and f). Porphyritic texture is the main texture in hbl-andesite rock samples exhibited by both plagioclase and hornblende minerals (Fig. 3d-h). The groundmass comprises micro-phenocrysts and microlites of plagioclase, hornblende, sanidine, and hematite minerals in the hbl-andesite rock samples (Fig. 3g).

Despite the fact that all magmatic minerals within andesitic rocks from WV preserved their magmatic nature and appearances, it's concluded that the primary alteration product includes only sericite after plagioclase and sanidine (Fig. 3a-f).

4.2 Mineralogy

Detailed mineralogical studies for the andesitic rocks in the Mawat area via XRD analysis shows that the andesitic rocks within studied area comprise different phases, such as albite, pyroxene, hornblende, quartz, and hematite (Fig. 4a and b). Although the authors in the former sections classify the andesitic rocks into px-andesite and hbl-andesite, the pyroxene as a major phase is not detected via XRD analysis (Fig. 4a). This is may be due to the highly altered or replaced pyroxene with other minerals in the px-andesitic rocks. While hornblende as a major phase (21%) is detectable via XRD analysis in the hbl-andesite rock samples (Fig. 4b), this is consistence with the petrographical analysis too (Fig. 3d-h).

4.3 Geochemistry

For 10 samples of andesitic rock, major, trace element, and REE analysis have been acquired (Table 1). Specimens were often taken from the freshest areas of the andesitic bodies and major intrusions; for comparison, extra samples were gathered from the borders and nearby bodies of other igneous structures.

The preservation of andesitic textures, despite hydrothermal alterations, suggests minimal chemical changes. This is further evidenced by the whole rock geochemical analysis, which confirms the andesitic nature of the samples. This might be due to the low concentrations of LOI, which support the freshness of all andesitic rock samples (LOI <4.5 is said to be unaltered samples, after Polat and Hofmann (2003).

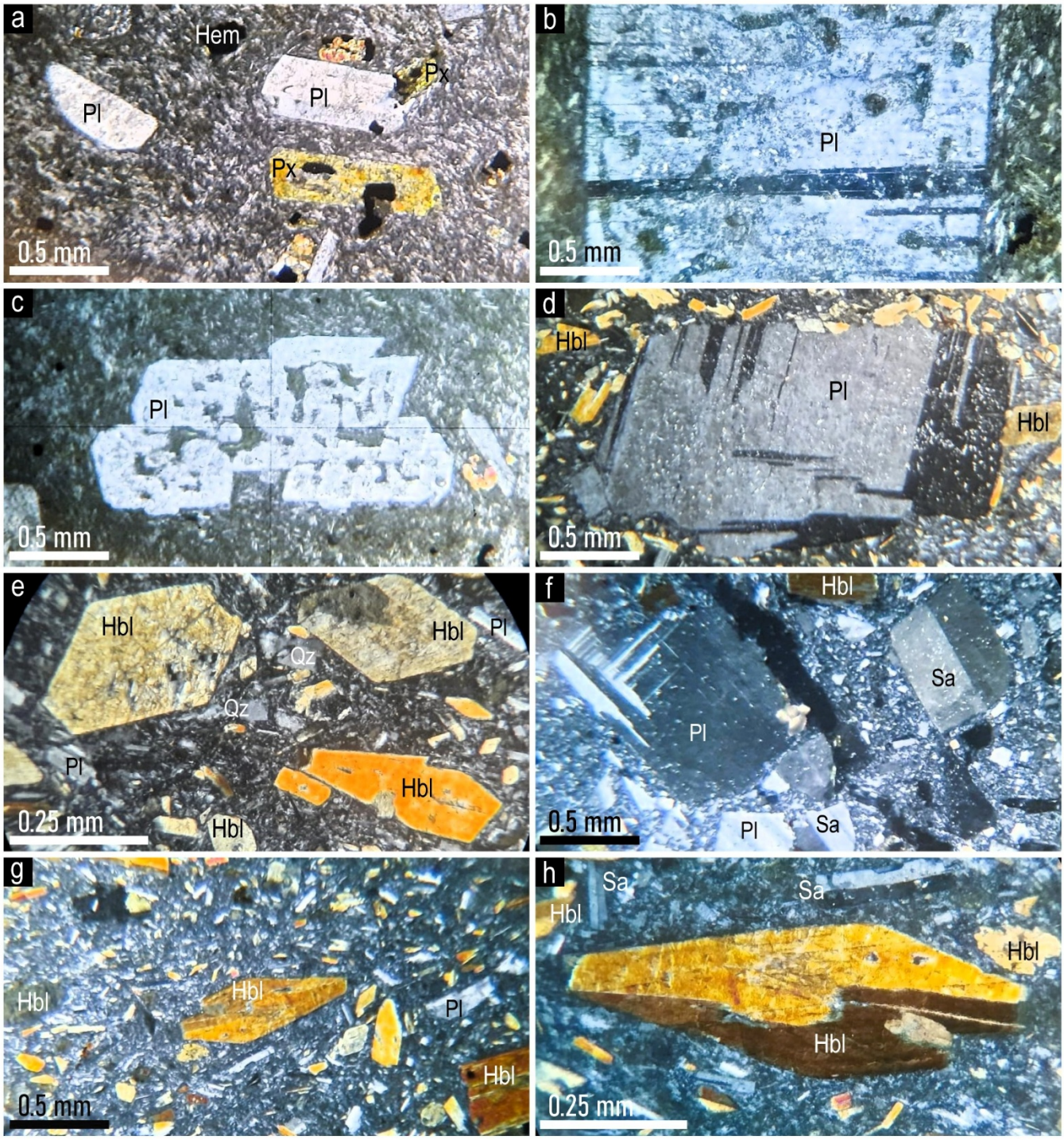

Figure 3. (a-c) Pyroxene andesite with platy, sieved texture plagioclase phenocrysts; (e-h) Hornblende andesite dominated by plagioclase and hornblende phenocrysts.

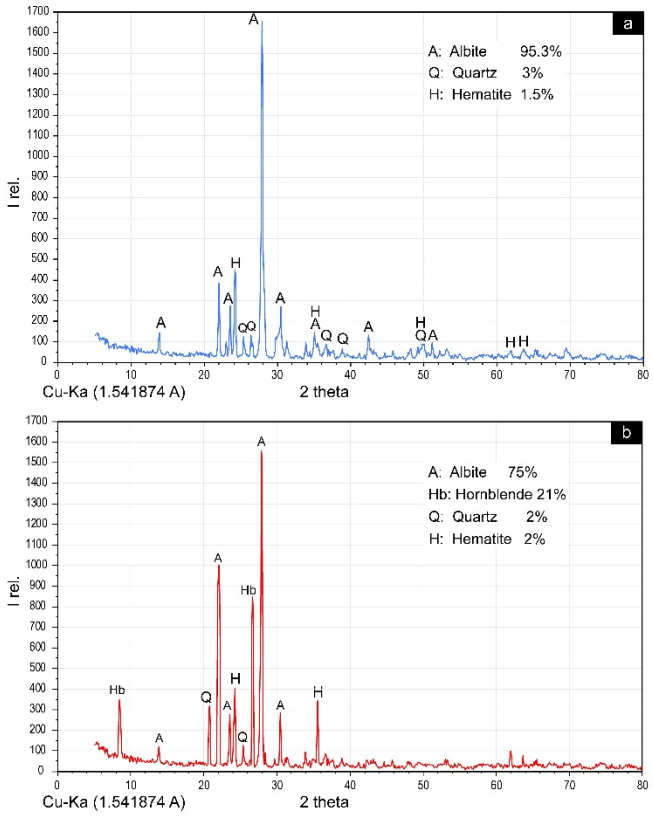

Figure 4. X-Ray diffraction patterns for the andesitic rocks in Mawat area, (a) Pyroxene andesite, (b) Hornblende andesite.

Whole rock geochemical analysis confirms the andesitic nature of all samples within WVsg, with SiO_2 contents ranging from 59.9 to 62 wt.% for pyroxene andesites and 61.6 to 63 wt.% for hornblende andesites. In general, pyroxene andesite rock samples are characterized slightly lower concentrations of CaO and K_2O and slightly higher concentrations of Al_2O_3, Fe_2O_3, MgO, Na_2O, and TiO_2 compared to the hornblende andesite rock samples (Table. 1).

Major element Harker diagrams for all oxides are plotted against SiO_2 (Fig. 5). Major element contents such as Al_2O_3, Fe_2O_3, MgO, Na_2O, TiO_2, MnO, and P_2O_5 are decreased with increasing SiO_2 content and may indicative of in situ fractional crystallizations of plagioclase (albite), pyroxene, and hornblende. While contents like, K_2O, and CaO are increased with increasing SiO_2 content (Fig. 5).

Using TAS classification diagrams of LeBas et al. (1986), all rock samples exhibit andesitic composition and represented by calc-alkaline towards the high-K calc-alkaline magmatic series (Fig. 6). Furthermore, the REE diagram normalized to REE of Upper Continental Crust (Taylor & McLennan, 1995) shows a slight depletion of LREE in pyroxene andesite rock samples and no significant changes in the HREE pattern. While hornblende andesite rock samples show depletion patterns of both LREE and HREE if compared to the REE of upper continental crust and exhibit a pronounced positive Eu anomaly, indicating enrichment in europium relative to neighboring Sm and Gd rare earth elements (Fig. 7).

The average Mg# value of the andesitic rock samples is 47.69 (Table 1), which is compatible with High-Mg andesites rather than normal arc magma and or mantle-derived magma melts (Kelemen, 1995) (Fig. 8a). Furthermore, the Ce/Pb ratios of the andesitic rock samples range from 4.05 to 11.3, which are lower than the predicted values for Mantle-derived melts (Hofmann, 1988) (Fig. 8b).

5. Discussions

Andesitic rocks within WVSg in the Mawat area have been classified into two types, px-andesites and hbl-andesites. This classification is based on the field, petrography, mineralogy, and geochemical differences in these rock types. The studied andesite rocks in the WV exhibit petrographic characteristics indicative of andesitic intrusion in the Mawat area (Fig. 3). The primary mineral assemblages (pyroxene-plagioclase-sanidine for px-andesites and hornblende-plagioclase-sanidine for hbl-andesites) with pilotasitic to trachytic and porphyritic textures suggest crystallization from a calc-alkaline magma. Differences in mineral assemblages and textures of the px-andesites and hbl-andesites indicate a heterogeneity of the magmatic sources for these andesite rocks.

Table 1. Whole rock major, trace and REE concentrations (ICP-MS) for the Andesitic rocks.

Sample names	A-M1	A-M2	A-M3	A-M4	A-M5	A-M6	A-M7	A-M8	A-M9	A-M10	D.L.	Average
Rock type	Px-Andesite	Px-Andesite	Px-Andesite	Px-Andesite	Px-Andesite	Hbl-Andesite	Hbl-Andesite	Hbl-Andesite	Hbl-Andesite	Hbl-Andesite		Mean
Oxides (Wt.%)												
SiO_2	60.30	60.80	59.90	62.00	61.20	63.00	62.30	62.70	62.80	61.60	<0.01	61.66
Al_2O_3	16.40	16.30	17.20	15.30	16.00	14.10	14.50	14.20	13.90	15.40	<0.01	15.33
Fe_2O_3	5.04	5.32	5.67	4.92	5.18	3.28	3.90	3.62	3.15	4.00	<0.01	4.41
CaO	2.76	2.70	2.15	3.80	3.20	5.05	4.88	5.12	5.25	4.00	<0.01	3.89
MgO	2.40	2.45	2.78	2.10	2.35	1.52	1.65	1.72	1.38	2.00	<0.01	2.04
Na_2O	5.83	5.95	6.12	5.30	5.88	4.78	4.65	4.52	4.85	5.00	<0.01	5.29
K_2O	1.78	1.92	1.50	2.10	1.95	2.32	2.15	2.20	2.45	2.12	<0.01	2.05
TiO_2	0.89	0.90	1.02	0.65	0.80	0.22	0.38	0.35	0.30	0.60	<0.01	0.61
MnO	0.09	0.10	0.11	0.08	0.09	0.06	0.07	0.05	0.04	0.06	<0.01	0.08
P_2O_5	0.25	0.28	0.31	0.22	0.26	0.13	0.11	0.09	0.08	0.18	<0.01	0.19
LOI	2.63	2.9	2.5	3.5	3	4.28	3.6	3.9	4.1	3.2	<0.01	3.36
Total	**98.37**	**99.62**	**99.26**	**99.97**	**99.91**	**98.74**	**98.19**	**98.47**	**98.3**	**98.16**		**98.89**
Mg#	48.54	47.86	47.71	45.60	49.27	48.49	45.82	46.46	47.33	49.76		47.69
Trace (ppm)												
Ag	<0.5	<0.5	<0.5	<0.5	<0.5	<0.5	<0.5	<0.5	<0.5	<0.5	0.01-1	<0.5
As	<5	<5	<5	<5	<5	<5	<5	<5	<5	<5	5	*Bdl*
Cd	<0.5	<0.5	<0.5	<0.5	<0.5	<0.5	<0.5	<0.5	<0.5	<0.5	0.01-1	<0.5
Co	13	12	13	12	11	6	6	5	7	6	0.01-1	9.1
Cr	40	35	28	45	38	190	205	220	240	195	5	123.6
Ni	15	12	10	18	14	34	38	42	48	36	0.01-1	26.7
Cu	22	25	28	20	23	5	6	4	3	5	0.01-1	14.1
Li	10	11	12	10	11	10	9	8	7	9	0.01-1	9.7
Mo	<1	<1	<1	<1	<1	1	1	1	1	1	0.01-1	1.0
Sn	2	2	2	2	2	<1	<1	<1	<1	<1	0.01-1	2.0
Pb	8	9	10	7	8	2	3	3	4	3	0.01-1	5.7
Sc	10	11	12	10	11	9	8	7	6	8	0.01-1	9.2
Tl	<10	<10	<10	<10	<10	<10	<10	<10	<10	<10	0.01-1	<10
Zn	61	65	70	58	63	31	34	29	27	33	0.01-1	47.1
Ba	401	435	467	385	420	348	325	310	365	335	0.01-1	379.1
Rb	35.8	38.2	41.5	33.2	36.5	23.8	21.5	19.8	25.4	22.6	0.01-1	29.8
Sr	402	385	365	415	395	500	520	535	485	510	0.01-1	451.2
Th	6.66	7.12	7.95	6.12	6.88	2.42	2.15	1.88	1.65	2.28	0.01-1	4.5
Nb	17.6	18.2	19.5	16.8	17.9	3.8	4.2	3.5	2.9	4	0.01-1	10.8
Hf	5.2	5.6	6	4.8	5.4	2.6	2.4	2.3	2.1	2.5	0.01-1	3.9
Ta	1.2	1.35	1.5	1.05	1.25	0.3	0.35	0.28	0.25	0.32	0.01-1	0.8
Ga	19	20	21	18.5	19.5	16.6	17.2	16.8	15.8	17	0.01-1	18.1
Cs	0.13	0.15	0.18	0.14	0.16	0.22	0.2	0.18	0.25	0.21	0.01-1	0.2
U	2.3	2.55	2.8	2.15	2.45	0.67	0.72	0.65	0.55	0.7	0.01-1	1.6
V	96	105	112	99	102	87	92	95	82	90	0.01-1	96.0
W	1	1	1	1	1	<1	<1	<1	<1	<1	0.01-1	1.0
Y	22.3	24.1	26.7	20.8	23.5	8.5	7.8	6.9	5.6	8.2	0.01-1	15.4
Zr	236	265	290	200	250	111	105	98	85	170	0.01-1	181.0
REE (ppm)												
La	21.9	23.5	25.3	20.4	22.7	10.7	9.8	8.9	7.5	10.2	0.01-1	16.09
Ce	43.6	47.1	50.4	41.2	45.3	22.6	20.8	18.9	16.2	21.5	0.01-1	32.76
Pr	4.99	5.45	5.85	4.75	5.25	2.76	2.55	2.35	2.05	2.65	0.01-1	3.87
Nd	19.8	21.2	22.8	18.6	20.5	11.7	10.9	10.2	9.1	11.2	0.01-1	15.60
Sm	4.58	4.92	5.25	4.25	4.75	2.53	2.35	2.15	1.85	2.45	0.01-1	3.51
Eu	1.18	1.12	1.25	1	1.05	0.71	0.85	0.8	0.73	0.9	0.01-1	0.96
Gd	3.99	4.25	4.55	3.85	4.1	2.33	2.15	2.05	1.75	2.25	0.01-1	3.13
Tb	0.64	0.71	0.78	0.6	0.68	0.27	0.25	0.22	0.18	0.26	0.01-1	0.46
Dy	4.03	4.35	4.75	3.85	4.15	1.54	1.45	1.35	1.15	1.5	0.01-1	2.81
Ho	0.81	0.88	0.95	0.75	0.82	0.28	0.25	0.22	0.18	0.24	0.01-1	0.54
Er	2.19	2.38	2.65	2.05	2.25	0.87	0.78	0.72	0.65	0.8	0.01-1	1.53
Tm	0.34	0.38	0.42	0.32	0.36	0.12	0.11	0.1	0.08	0.12	0.01-1	0.24
Yb	2.49	2.75	3.05	2.35	2.65	0.97	0.85	0.78	0.65	0.9	0.01-1	1.74
Lu	0.37	0.4	0.45	0.35	0.38	0.15	0.14	0.12	0.1	0.13	0.01-1	0.26
Ce/Pb	5.45	5.23	5.04	5.89	5.66	11.30	6.93	6.30	4.05	7.17		6.30
Sr/Y	18.03	15.98	13.67	19.95	16.81	58.82	66.67	77.54	86.61	62.20		43.63

*Mg# = molar Mg / (Molar Mg + Molar Fe) *100)* *LOI: Loss On Ignition* *Bdl: Below detection limit*

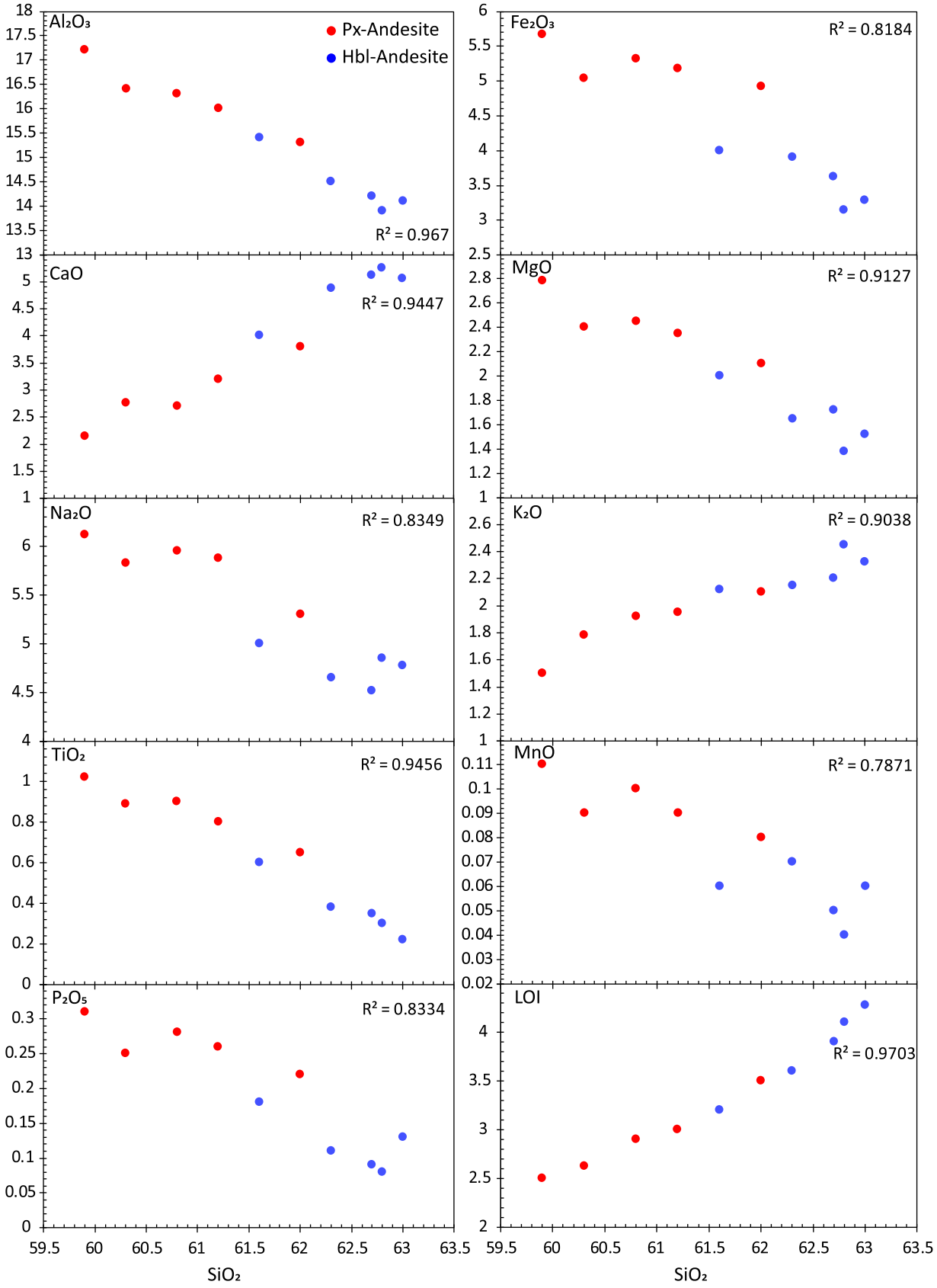

Figure 5. Harker diagrams for major oxides in andesitic rocks from Mawat area.

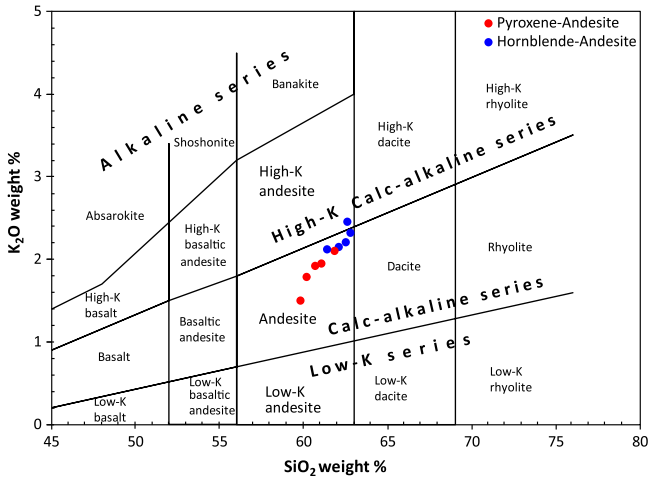

Figure 6. TAS classification diagrams for andesitic rocks represented by Calc-alkaline towards High-K Calc-Alkaline magmatic series (LeBas et al., 1986).

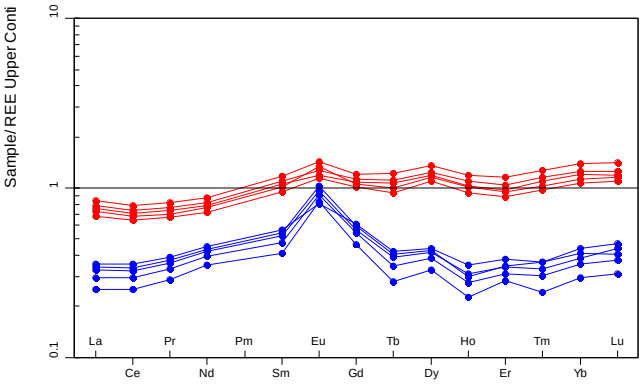

Figure 7. Normalized REE patterns of andesitic rock samples/ REE of Upper Continental Crust in the Mawat area, normalizations are after Taylor and McLennan (1995). Symbols are the same as in Figures 4 and 5.

5.1 Adakitic signature for Walash andesites

According to the literature reviews on volcanic rocks within WVSg, almost all of literature has repeatedly revealed a tholeiitic to calc-alkaline signature in the various volcanic rocks, indicating subduction zone magmatism-related origins (Aziz, 1986; Ali et al., 2013; Aswad et al., 2013; Mohammed and Qaradaghi, 2016; Qaradaghi & Mirza, 2023; Qaradaghi, 2024). However, adakite or adakitic rocks are intermediate to felsic rocks with unique geochemical features, including high sodium content (3.5-7.5 wt.% Na_2O), high aluminum content (Al_2O_3 > 15 wt.%), and elevated strontium levels (Sr > 400 ppm), according to (Castillo, 2012). Furthermore, according to (Defant and Drummond, 1990), these rocks develop when young (<25 Ma) subducting oceanic crust melts partially along convergent margins. Adakites are also distinguished by their high silica content and Sr/Y and La/Yb ratios in volcanic and plutonic environments. They can form in a variety of tectonic settings, including subduction zones, continental collision zones, and extensional continental environments, and are impacted by a number of petrogenetic processes, as described by many research (Defant & Drummond, 1990; Defant & Kepezhinskas, 2001; Huang & He, 2010; Sun et al., 2012; Luchitskaya, 2022).

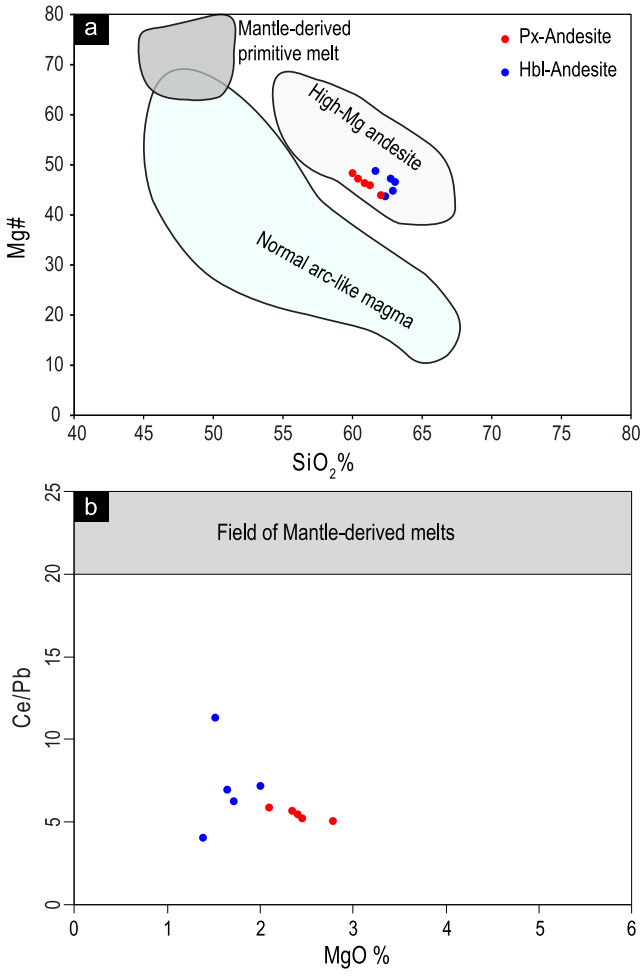

Figure 8. Binary diagrams show andesitic rocks located outside of the Mantle derived primitive melts (a) Mg# vs SiO_2 after Kelemen (1995). (b) Ce/Pb vs MgO% after Hofmann (1988).

A number of broadly accepted models have been proposed to explain the origin of adakites: (1) melting of a subducted oceanic slab (Defant & Drummond, 1990; Condie, 2005; Hernández-Uribe et al., 2020); (2) melting of a delaminated ancient lower crust (Castillo, 2012; Qian & Hermann, 2013); (3) melting of a thickened mafic lower crust (Chung et al., 2003; Ma et al., 2015); (4) fractional crystallization of basic magmas (Chiaradia, 2009; Xu et al., 2022); and (5) mélange diapir in subduction zone (Yan et al., 2019; Wang et al., 2024). In general, adakites created by melting of subducted oceanic slab or delaminated lower crust are characterized by high Mg# values and high concentrations of Cr and Ni because they are predicted to have interacted with peridotite as they moved through the mantle (Defant & Drummond, 1990; Kelemen, 1995; Luchitskaya, 2022).

Accordingly, Mg# is a helpful index for distinguishing distinct melt origins, according to experimental studies (Kelemen, 1995; Danyushevsky et al., 2002; Zhong et al., 2017). Melts from the basaltic lower crust have low Mg# (<40) regardless of melting degree, while Mg# > 40 requires the presence of a mantle component (Rapp & Watson, 1995; Rapp et al., 2010). Thus, the hbl-andesite in the Walash volcanics displays relatively high Mg# values (45.82–49.76, with average of 47.65) and high concentrations of Cr (190–240 ppm, with average of 210 ppm) and Ni (34–48 ppm, averaging 39.6 ppm) (Table 1), supporting the first and second genetic models of their genetic origin. Regarding the px-andesite rock samples, the fourth model (fractional crystallization of basic magmas) is more preferable. Considering the following reasons: (1) mineralogical composition of px-andesite rock samples (Figs. 3a and 4a); (2) the presence of linear correlations of selected major elements against SiO_2 (Fig. 5); (3) coeval mafic and intermediate igneous rocks have been discovered in the Walash volcanics and adjacent areas of Mawat. Thus, exceed fractional crystallization of basic magmas could generate andesitic intrusions with such geochemistry (e.g., Chiaradia, 2009; Li et al., 2022; Saikia et al., 2022).

Furthermore, px-andesites and hbl-andesites in the WV are characterized by higher trace elemental ratios like Ba/Nb and La/Nb than those of depleted mantle-derived melts such as MORB and OIB (e.x., Sun & McDonough, 1989). Thus, the Ba/Nb versus La/Nb diagram of Jahn et al. (1999) indicates a variation range of volcanic arc setting for both px-andesite and hbl-andesite rocks of the Mawat area (Fig. 9a). While trace elemental ratios of Sr/Y versus Y diagram indicate a normal calc-alkaline andesitic magma suite for px-andesite rock samples and an adakite-like andesitic magma suite for hbl-andesite rock samples (Fig. 9b).

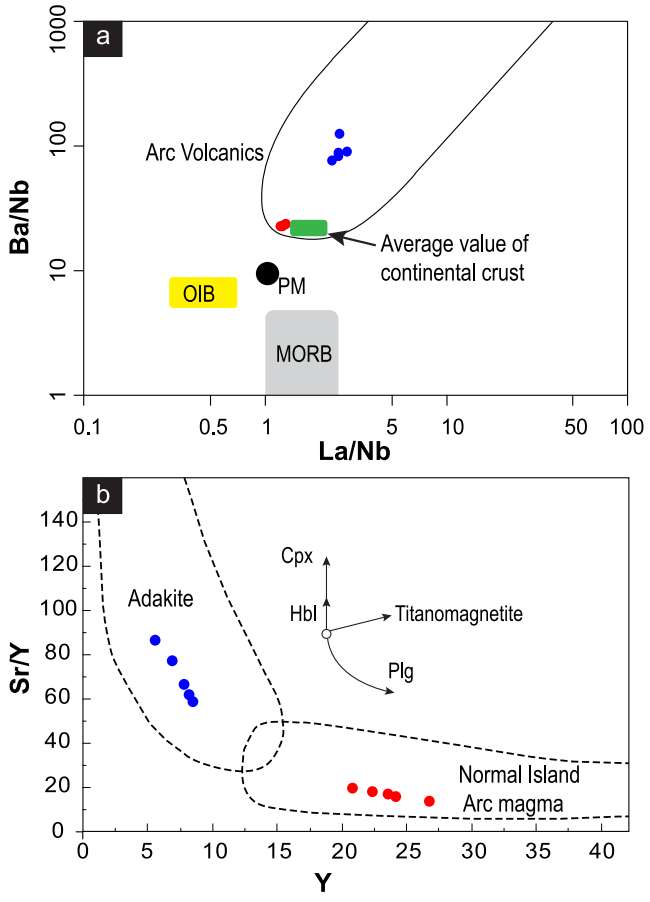

Figure 9. (a) La/Nb vs. Ba/Nb diagram showing very high Ba/Nb and La/Nb ratios of andesitic rocks in the Mawat area. Data sources: Arc volcanics and average continental crust fields are after Jahn et al. (1999); PM, OIB, and MORB are after Sun and McDonough (1989). (b) Sr/Y vs. Y diagram showing normal andesitic magma for px-andesite and adakite-like magma for hbl-andesite rock samples. Symbols are the same as in Figures 4 and 5.

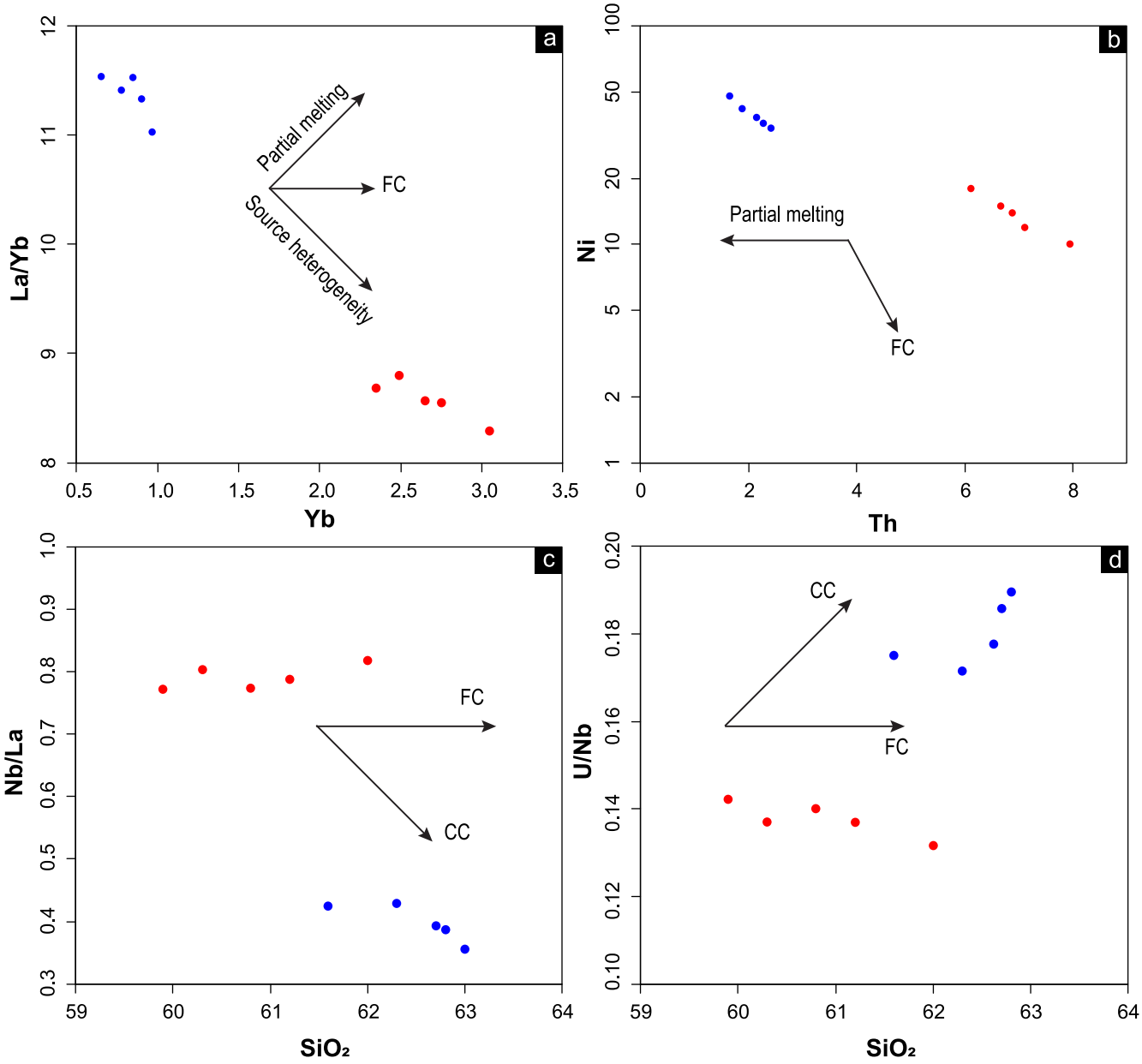

Figure 10. (a) La/Yb vs Yb diagram showing source heterogeneity of andesitic rocks from WV, magmatic rends are after Fan et al. (2004); (b) Ni vs Th plot, showing dominant role of fractional crystallization magmatic process, magmatic trends are after (Fan et al., 2004); (c) and (d) Nb/La and U/Nb vs SiO_2 diagrams showing fractional crystallization rend for px-andesites and Crustal contamination trend for hbl-andesite rock samples, trends are after Ye et al. (2018). Symbols are the same as in Figures 4 and 5.

5.2 Magmatic source

The geochemical systematics of the investigated andesites form the WV imply that they are the result of a compositionally varied magmatic source and different evolutionary processes. The La/Yb against Yb (Fig. 10a) shows that both pyroxene- and hornblende-bearing andesites are not the result of a consistent mantle source. Instead, the observed spread is the result of input from variably enriched mantle sources, most likely a subduction-modified

lithospheric mantle with inherent trace element composition heterogeneity.

The Ni vs Th binary diagram further constrains fractionation processes, as the compositional array is compatible with fractional crystallization (FC) rather than partial melting (PM) (Fig. 10b). The systematic loss of Ni with accompanying enrichment in Th is diagnostic of successive removal of early-crystallizing mafic phases, supporting the hypothesis that differentiation, rather than primary melt production, governed the geochemical development of the Walash andesites.

Discrimination using Nb/La and U/Nb versus SiO_2 systematics provides more information (Fig. 10 c and d). The px-andesite rock samples exhibit a consistent trend that can be attributed to fractional crystallization, indicating that closed-system magmatic differentiation with minimal crustal interaction dominated their evolution. The hbl-andesite rock samples, on the other hand, fall closer to the array of crustal contamination. Assimilation of continental crustal material during magma ascent or settlement is indicated by their enhanced SiO_2 concentrations and U enrichment relative to Nb. The hydrous nature of hornblende-bearing magmas, which are more likely to be held in mid- to upper-crustal reservoirs, supports this hypothesis and increases the possibility of crustal assimilation (Collins et al., 2020; Kawaraṅ et al., 2025). As mentioned earlier, the Hbl-andesites exhibit an adakitic geochemical signature. However, trace-element systematics (e.g., Nb/La and U/Nb versus SiO_2; Fig. 10c and d) indicate a significant role for crustal contamination. Therefore, the author interprets the high Sr/Y and La/Yb ratios not solely as evidence of direct slab melting but rather as the result of assimilation of lower-crustal material by a mantle-derived magma. This model simultaneously accounts for the adakitic signature, the high Mg# and compatible-element concentrations (reflecting mantle interaction), and the clear trends of crustal contamination.

Several other trace elemental ratios have been traced versus La/Sm ratios to investigate FC, AFC and Mixing models after (Szilas et al., 2017), the pyroxene andesite rock samples more coincide with FC and AFC models of fractionation while hornblende andesites more prefer the mixing models between two mafic and felsic magma, figure are not presented in this context.

These geochemical connections taken together imply that both andesite groups were changed by fractional crystallization after being derived from a diverse mantle source. The hbl-andesites, on the other hand, record additional crustal contributions, showing dual influences of differentiation and crustal assimilation in their petrogenesis, whereas the px-andesites maintain a dominantly fractional crystallization signature.

6. Conclusions

The following points are concluded in this study:

a. Two distinct types of andesitic rocks have been identified within the WVSg in the Mawat area: pyroxene-bearing andesites (px-andesites) and hornblende-bearing andesites (hbl-andesites). Their classification is supported by field observations, petrographic features, mineralogical composition, and geochemical characteristics.

b. The analyzed andesitic rocks display elevated LILE/HFSE and LREE/HREE ratios, indicating their derivation from magmas associated with subduction-related environments.

c. The px-andesites were generated primarily through fractional crystallization, whereas the hbl-andesites reflect the influence of crustal contamination during magma evolution.

d. Geochemically, the px-andesites represent typical calc-alkaline magmas, while the hbl-andesites exhibit adakitic affinities.

In summary, the integration of field, petrographic, and ICP-MS geochemical data effectively characterizes the petrogenetic evolution of the WVSg andesites and clarifies their tectono-magmatic context within the northeastern Arabian Plate.

Conflict of interest

The author declares that there are no conflicts of interest pertaining to this manuscript.

CRediT authorship contribution statement

Jabbar Qaradaghi performed the entire research and writing associated with this manuscript.

Acknowledgments

The author expresses his gratitude to the earth sciences and petroleum department at Sulaimani University for their assistant in lab acquisition for sample preparation (powdering) for geochemical analysis.

References

Al-Kadhimi, J., Sissakian, V., Fattah, A., & Deikran, D. (1996). Tectonic Map of Iraq, 2nd edit., scale 1: 1000 000. GEOSURV, Baghdad, Iraq.

Al-Qayim, B., Omer, A., & Koyi, H. (2012). Tectonostratigraphic overview of the Zagros suture zone, Kurdistan region, Northeast Iraq. [Research Article]. GeoArabia, 17(4), 109-156.

Ali, S. A., Buckman, S., Aswad, K. J., Jones, B. G., Ismail, S. A., & Nutman, A. P. (2013). The tectonic evolution of a Neo-Tethyan (Eocene–Oligocene) island-arc (Walash and Naopurdan groups) in the Kurdistan region of the Northeast Iraqi Zagros Suture Zone. Island Arc, 22(1), 104-125.

Aswad, K. J. A., Al-Samman, A. H. M., Aziz, N. R. H., & Koyi, A. M. A. (2013). The geochronology and petrogenesis of Walash volcanic rocks, Mawat nappes: constraints on the evolution of the northwestern Zagros suture zone, Kurdistan Region, Iraq. Arabian Journal of Geosciences, 7(4), 1403-1432. https://doi.org/10.1007/s12517-013-0873-x

Aziz, N. R. (1986). Petrochemistry, petrogenesis and tectonic setting of spilitic rocks of Walash volcano sedimentary group in Qala-Diza area, NE Iraq. Unpub [MSc Thesis, Mosul].

Bolton, C. (1958). The geology of the Ranya area. Manuscript report No. 271. GEOSURV, Baghdad.

Buday, T., & Jassim, S. (1987). The regional geology of Iraq, vol. 2: tectonism, magmatism and metamorphism. GEOSURV, Baghdad, 352pp.

Cassidy, M., Edmonds, M., Watt, S. F., Palmer, M. R., & Gernon, T. M. (2015). Origin of basalts by hybridization in andesite-dominated arcs. Journal of Petrology, 56(2), 325-346.

Castillo, P. R. (2012). Adakite petrogenesis. Lithos, 134, 304-316.

Chen, L., Zheng, Y.-F., Xu, Z., & Zhao, Z.-F. (2021). Generation of andesite through partial melting of basaltic metasomatites in the mantle wedge: Insight from quantitative study of Andean andesites. Geoscience Frontiers, 12(3), 101124.

Chiaradia, M. (2009). Adakite-like magmas from fractional crystallization and melting-assimilation of mafic lower crust (Eocene Macuchi arc, Western Cordillera, Ecuador). Chemical geology, 265(3-4), 468-487.

Chung, S.-L., Liu, D., Ji, J., Chu, M.-F., Lee, H.-Y., Wen, D.-J., Lo, C.-H., Lee, T.-Y., Qian, Q., & Zhang, Q. (2003). Adakites from continental collision zones: melting of thickened lower crust beneath southern Tibet. Geology, 31(11), 1021-1024.

Collins, W. J., Murphy, J. B., Johnson, T. E., & Huang, H.-Q. (2020). Critical role of water in the formation of continental crust. Nature Geoscience, 13(5), 331-338.

Condie, K. C. (2005). TTGs and adakites: are they both slab melts? Lithos, 80(1-4), 33-44.

Danyushevsky, L. V., McNeill, A. W., & Sobolev, A. V. (2002). Experimental and petrological studies of

melt inclusions in phenocrysts from mantle-derived magmas: an overview of techniques, advantages and complications. Chemical geology, 183(1-4), 5-24.

Davidson, J., Turner, S., Handley, H., Macpherson, C., & Dosseto, A. (2007). Amphibole "sponge" in arc crust? Geology, 35(9), 787-790.

Defant, M. J., & Drummond, M. S. (1990). Derivation of some modern arc magmas by melting of young subducted lithosphere. nature, 347(6294), 662-665.

Defant, M. J., & Kepezhinskas, P. (2001). Evidence suggests slab melting in arc magmas. Eos, Transactions American Geophysical Union, 82(6), 65-69.

Erdmann, S., Chen, L. H., Liu, J. Q., Xue, X. Q., & Wang, X. J. (2019). Hot, volatile-poor, and oxidized magmatism above the stagnant Pacific plate in Eastern China in the Cenozoic. Geochemistry, Geophysics, Geosystems, 20(11), 4849-4868.

Fan, W.-M., Guo, F., Wang, Y.-J., & Zhang, M. (2004). Late Mesozoic volcanism in the northern Huaiyang tectono-magmatic belt, central China: partial melts from a lithospheric mantle with subducted continental crust relicts beneath the Dabie orogen? Chemical geology, 209(1-2), 27-48.

Gao, M.-H., Liu, P.-P., Chung, S.-L., Li, Q.-L., Wang, B., Tian, W., Li, X.-H., & Lee, H.-Y. (2022). Himalayan zircons resurface in Sumatran arc volcanoes through sediment recycling. Communications Earth & Environment, 3(1), 283.

Gill, J. B. (2012). Orogenic andesites and plate tectonics (Vol. 16). Springer Science & Business Media.

Gill, R., & Fitton, G. (2022). Igneous rocks and processes: a practical guide. John Wiley & Sons.

Hernández-Uribe, D., Hernández-Montenegro, J. D., Cone, K. A., & Palin, R. M. (2020). Oceanic slab-top melting during subduction: Implications for trace-element recycling and adakite petrogenesis. Geology, 48(3), 216-220.

Hofmann, A. W. (1988). Chemical differentiation of the Earth: the relationship between mantle, continental crust, and oceanic crust. Earth and planetary science letters, 90(3), 297-314.

Huang, F., & He, Y. (2010). Partial melting of the dry mafic continental crust: implications for petrogenesis of C-type adakites. Chinese Science Bulletin, 55, 2428-2439.

Jahn, B.-m., Wu, F., Lo, C.-H., & Tsai, C.-H. (1999). Crust–mantle interaction induced by deep subduction of the continental crust: geochemical and Sr–Nd isotopic evidence from post-collisional mafic–ultramafic intrusions of the northern Dabie complex, central China. Chemical geology, 157(1-2), 119-146.

Jassim, S. Z., & Goff, J. C. (2006). Geology of Iraq. DOLIN, sro, distributed by Geological Society of London.

Kawaraṅ, H., Matsumoto, M., & Kuritani, T. (2025). Generation of andesitic–dacitic magmas by open-system progressive melting of the middle crust in Rishiri Volcano, northern Japan. Lithos, 108221.

Kelemen, P., Hanghøj, K., & Greene, A. (2003). One view of the geochemistry of subduction-related magmatic arcs, with an emphasis on primitive andesite and lower crust. Treatise on geochemistry, 3, 659.

Kelemen, P. B. (1995). Genesis of high Mg# andesites and the continental crust. Contributions to Mineralogy and Petrology, 120(1), 1-19.

Koyi, A. (2009). Sr-Nd isotopical significance of Walash volcanic rocks, Mawat area, NE Iraq. Zanco J Pure Sci Salahaddin University, Hawler, 21, 39-45.

LeBas, M., Maitre, R. L., Streckeisen, A., Zanettin, B., & Rocks, I. S. o. t. S. o. I. (1986). A chemical classification of volcanic rocks based on the total alkali-silica diagram. Journal of Petrology, 27(3), 745-750.

Li, C., Niu, M., Yuan, X., Yan, Z., Wu, Q., Li, X., & Sun, Y. (2022). Geochemical signals of coexisting magma

mixing and fractional crystallization processes in the arc setting: Case study of Wulan intrusive suite in the NE Tibet Plateau. Lithos, 432, 106914.

Luchitskaya, M. (2022). The composition, petrogenesis, and geodynamic setting of adakite magmatism: An overview. Geotectonics, 56(4), 486-519.

Ma, Q., Zheng, J.-P., Xu, Y.-G., Griffin, W. L., & Zhang, R.-S. (2015). Are continental "adakites" derived from thickened or foundered lower crust? Earth and planetary science letters, 419, 125-133.

Mibe, K., Kawamoto, T., Matsukage, K. N., Fei, Y., & Ono, S. (2011). Slab melting versus slab dehydration in subduction-zone magmatism. Proceedings of the National Academy of Sciences, 108(20), 8177-8182.

Mohammad, Y. O., Cornell, D. H., Qaradaghi, J. H., & Mohammad, F. O. (2014). Geochemistry and Ar–Ar muscovite ages of the Daraban Leucogranite, Mawat Ophiolite, northeastern Iraq: implications for Arabia–Eurasia continental collision. Journal of Asian Earth Sciences, 86, 151-165. https://doi.org/10.1016/j.jseaes.2013.09.029

Mohammad, Y. O., and Qaradaghi, J. H. (2016). Geochronological and mineral chemical constraints on the age and formation conditions of the leucogranite in the Mawat ophiolite, Northeastern of Iraq: insight to sync-subduction zone granite. Arab J Geosci 9, 608. https://doi.org/10.1007/s12517-016-2630-4

Polat, A., & Hofmann, A. (2003). Alteration and geochemical patterns in the 3.7–3.8 Ga Isua greenstone belt, West Greenland. Precambrian Research, 126(3-4), 197-218.

Qaradaghi, J. M. A. (2024). Genesis and Tectonics of Basaltic Pillow lava and Peperites within Walash Volcano-sedimentary group, Mawat area, Iraqi Kurdistan Region [Ph.D. Thesis, University of Sulaimani]. University of Sulaimani.

Qaradaghi, J. M. A., & Mirza, T. A. (2023). Peperites: Insight into the Submarine Eruptions within Walash Volcanosedimentary Group, Mawat Area, Iraqi Kurdistan Region. ARO: The Scientific Journal of Koya University, 11(2). https://doi.org/10.14500/aro.11363

Qaradaghi, J. M., Mohammed, Y. O., and Aziz, S. A., (2019). Petrology and Geochemistry of Gole Pillow Basalt in Penjween area Kurdistan Region-NE Iraq. Tikrit Journal of Pure Science, 24(7), 66-81. https://doi.org/10.25130/tjps.v24i7.460

Qian, Q., & Hermann, J. (2013). Partial melting of lower crust at 10–15 kbar: constraints on adakite and TTG formation. Contributions to Mineralogy and Petrology, 165(6), 1195-1224.

Rapp, R., Norman, M., Laporte, D., Yaxley, G., Martin, H., & Foley, S. (2010). Continent formation in the Archean and chemical evolution of the cratonic lithosphere: melt–rock reaction experiments at 3–4 GPa and petrogenesis of Archean Mg-diorites (sanukitoids). Journal of Petrology, 51(6), 1237-1266.

Rapp, R. P., & Watson, E. B. (1995). Dehydration melting of metabasalt at 8–32 kbar: implications for continental growth and crust-mantle recycling. Journal of Petrology, 36(4), 891-931.

Reubi, O., & Müntener, O. (2022). Making Andesites and the Continental Crust: Mind the Step When Wet. Journal of Petrology, 63(6). https://doi.org/10.1093/petrology/egac044

Ruiz-Mendoza, V., Verma, S. K., Torres-Sánchez, D., Barry, T. L., Moreno, J. A., & Torres-Hernández, J. R. (2021). Geochemistry and geochronology of intermediate volcanic rocks from the Compostela area, Nayarit, Mexico: Implications for petrogenesis and tectonic setting. Geological Journal, 56(8), 4401-4428.

Saikia, A., Akhtar, S., & Negi, P. (2022). Role of fractional crystallization and partial melting in the generation of intermediate and acidic magmas of the Andaman Island Ophiolite suite of India. Geological Journal, 57(2), 906-924.

Straub, S. M., Gómez-Tuena, A., & Vannucchi, P. (2020). Subduction erosion and arc volcanism. Nature Reviews Earth & Environment, 1(11), 574-589.

Sun, S.-S., & McDonough, W. F. (1989). Chemical and isotopic systematics of oceanic basalts: implications for mantle composition and processes. Geological Society, London, Special Publications, 42(1), 313-345.

Sun, W.-D., Ling, M.-X., Chung, S.-L., Ding, X., Yang, X.-Y., Liang, H.-Y., Fan, W.-M., Goldfarb, R., & Yin, Q.-Z. (2012). Geochemical constraints on adakites of different origins and copper mineralization. The Journal of Geology, 120(1), 105-120.

Szilas, K., Tusch, J., Hoffmann, J. E., Garde, A. A., & Münker, C. (2017). Hafnium isotope constraints on the origin of Mesoarchaean andesites in southern West Greenland, North Atlantic Craton.

Tatsumi, Y., & Eggins, S. (1995). Subduction zone magmatism (Vol. 1). Wiley.

Taylor, S. R., & McLennan, S. M. (1995). The geochemical evolution of the continental crust. Reviews of geophysics, 33(2), 241-265.

Wang, X., Sun, M., Cai, K., Zhao, G., Xiao, W., Xia, X., & Li, P. (2024). Crustal recycling and growth via mélange diapir in subduction zones: Insights from two episodes of magmatism in the Northern Yili Block, NW China. Bulletin, 136(1-2), 774-792.

Xu, J., Xia, X.-P., Wang, Q., Spencer, C. J., Lai, C.-K., & Zhang, L. (2022). Two magma fractionation paths for continental crust growth: Insights from the adakite-like and normal-arc granites in the Ailaoshan fold belt (SW Yunnan, China). Bulletin, 134(11-12), 2986-3002.

Yan, H., Long, X., Li, J., Wang, Q., Zhao, B., Shu, C., Gou, L., & Zuo, R. (2019). Arc andesitic rocks derived from partial melts of mélange diapir in subduction zones: Evidence from whole-rock geochemistry and Sr-Nd-Mo isotopes of the Paleogene Linzizong volcanic succession in southern Tibet. Journal of Geophysical Research: Solid Earth, 124(1), 456-475.

Ye, X.-T., Zhang, C.-L., Wang, A.-G., Wu, B., & Wang, G.-D. (2018). Early Paleozoic slab rollback in the North Altun, Northwest China: New evidence from mafic intrusions and high-Mg andesites. Lithosphere, 10(6), 687-707.

Zhang, G., Zhang, J., Dalton, H., & Phillips, D. (2022). Geochemical and chronological constraints on the origin and mantle source of Early Cretaceous arc volcanism on the Gagua Ridge in western Pacific. Geochemistry, Geophysics, Geosystems, 23(9), e2022GC010424.

Zhong, Y., Chen, L.-H., Wang, X.-J., Zhang, G.-L., Xie, L.-W., & Zeng, G. (2017). Magnesium isotopic variation of oceanic island basalts generated by partial melting and crustal recycling. Earth and planetary science letters, 463, 127-135.